Werk

Jahr: 1977
Kollektion: fid.geo
Signatur: 8 Z NAT 2148:44
Digitalisiert: Niedersächsische Staats- und Universitätsbibliothek Göttingen
Werk Id: PPN1015067948_0044
PURL: http://resolver.sub.uni-goettingen.de/purl?PPN1015067948_0044

LOG Id: LOG_0047
LOG Titel: Stress and viscosity in the asthenosphere
LOG Typ: article

Übergeordnetes Werk

Werk Id: PPN1015067948
PURL: http://resolver.sub.uni-goettingen.de/purl?PPN1015067948
OPAC: http://opac.sub.uni-goettingen.de/DB=1/PPN?PPN=1015067948

Contact

Niedersächsische Staats- und Universitätsbibliothek Göttingen
Georg-August-Universität Göttingen
Platz der Göttinger Sieben 1
37073 Göttingen
Germany
Email: gdz@sub.uni-goettingen.de

J. Geophys. 44, 231–244, 1978

Journal of Geophysics

Stress and Viscosity in the Asthenosphere

U.R. Vetter

Institut für Geophysik der Universität Kiel, Neue Universität, D-2300 Kiel, Federal Republic of Germany

Abstract. Stresses and effective viscosities in the asthenosphere down to a depth of 400 km are calculated on the basis of the "temperature method". Oceanic and continental geotherms and two melting point-depth curves, the dry pyrolite solidus, and the Forsterite$_{90}$ melting curve are used for a conversion of temperature to viscosity. The dry pyrolite model results in high homologous temperatures in the asthenosphere (>0.9 below oceans), very low stresses (a few bar and lower), and a 300 km thick low viscosity zone. The Fo_{90} model has lower homologous temperatures; stresses in the asthenosphere are in the range of 5–100 bar, and the asthenosphere itself is not limited to a certain depth interval but extends to great depths.

Key words: Continental and oceanic asthenosphere – Melting-depth curves – Stresses – Effective viscosities.

1. Introduction

During the last 15 years progress has been made in laboratory study of the creep behavior of rocks. A number of experiments were conducted on the mineral olivine and olivine bearing rocks. It is the opinion of Goetze (in preparation), among others, that the orthorhombic mineral olivine of the approximate composition $(Mg_{0.91}Fe_{0.09})SiO_4$ is the dominant phase to about 350 km depth, where the transition to a spinel structure begins. Accordingly, it seems justified to ascribe tectonic movements in the depth range of 40–400 km to creep in olivine. This is certainly the case, since the other minerals (20–50%) which are found in the material of the uppermost mantle (pyroxene, spinel etc.) show a creep behavior in laboratory experiments which is not significantly different from that of olivine (Green and Radcliffe, 1972; Carter et al., 1972).

The results of laboratory measurements on olivine are described in papers by Carter and AvéLallemant (1970), Goetze and Brace (1972), Kirby and Raleigh

Contribution No. 157 of Institut für Geophysik, D-2300 Kiel

(1973), Post and Griggs (1973), Goetze and Kohlstedt (1973), Kohlstedt and Goetze (1974), Kohlstedt et al. (1976), and others. In the range of stresses (differential stresses $\sigma_1 - \sigma_3$) from 50 bar to about 10 kb and in a temperature field above $0.5\,T_m$ (T_m = melting temperature) the experimental data can be approximated by a power creep law of the general form

$$\dot{\varepsilon} = K\sigma^n \exp[(-Q + pV)/RT] \tag{1}$$

(Kohlstedt et al., 1976)

with $\dot{\varepsilon}$ = creep rate
K = constant
σ = shear stress (diff. stress)
Q = activation energy (for self diffusion of the slowest moving species)
V = the corresponding activation volume
p = lithostatic pressure
R = gas constant
T = temperature (in K).

The exponent n of the shear stress increases with increasing stress. For the stress range between 50 bar and about 2 kb a power creep law with an exponent $n = 3$ fits the data best. Creep in materials at very low stresses, i.e. about 1 bar and less, and at high temperatures ($> 0.75\,T_m$) is apparently transitional between that described by a power law ($= PL$) and Nabarro-Herring creep ($= NH$, with $n = 1$), which is a function of the grain size (Herring, 1950; Weertman, 1970; Kirby and Raleigh, 1973; Stocker and Ashby, 1973; Carter, 1976). Coble creep ($n = 1 - 2$) which has gained more acceptance recently (Twiss, 1976; Schwenn and Goetze, 1977) is not treated in this study.

Comparisons between experimentally and naturally deformed rock samples, by means of electron microscope observations, lead to the conclusion that the samples come from depths, where stresses from ca. 50 bar to 1 – 2 kb existed (Raleigh and Kirby, 1970; Nicolas et al., 1971; Phakey et al., 1972; Goetze and Kohlstedt, 1973; Carter, 1976; Nicolas, 1976). As pointed out by Meissner and Vetter (1976, in the following referred to as paper 1) regions from which these samples came may not be representative of the mantle in general, since some mechanism was operating there bringing up the samples to the surface, a process which is not common in the rest of the mantle. However, since stresses from 1 bar and smaller (in the middle of the asthenosphere) to a few kb (in the lithosphere) seem to cover the whole range of tectonic processes of creep and fracture (Vetter and Meissner, 1977; hereafter referred to as paper 2) the data obtained on laboratory and natural samples mentioned above should be applicable to the problem.

The creep rates in laboratory experiments are in general 8–10 orders of magnitude larger than geologic creep rates. An application of experimental data to in situ conditions requires an extrapolation to much lower creep rates (Kohlstedt et al., 1976; Goetze, in preparation). Moreover, the confining pressures in laboratory studies reach only 15 kb which corresponds to the upper

50 km. It has not yet been possible to detect any transition from *PL* to *NH* creep in rocks, neither under laboratory conditions nor in naturally deformed specimens.

Little is known about the exact composition of the silicate mixture which constitutes the upper mantle. Hence, melting point-depth relations are model dependent although the creep behavior of many mantle minerals seem to be similar as mentioned before. A further problem is the possible presence of fluid phases (water, carbon dioxide) which strongly surpress the melting point (Green and Liebermann, 1976). Because of the uncertainty in our knowledge of the fluid phases their effect on the melting point will not be considered in this study.

While in papers 1 and 2 some observational evidence for the transition from *PL* to *NH* creep was presented on the basis of uplift data, the present study attempts to define the range of conditions in which the different creep laws are valid. Hence, two models with different melting curves will be presented which are assumed to be the limiting cases for in situ conditions.

2. Models and Formulas Used

A plate tectonic model with an oceanic plate and a continental plate and their substructures to a depth of 400 km is considered (Fig. 1). Theoretical computations of the stress-depth distribution are performed for the model.

In Equation (1) the exponential term can be substituted for by a term including the diffusion coefficient. The influence of increasing pressure on the creep rate is taken into account by the increase of the melting temperature with pressure (Sherby and Simnad, 1961; Goetze and Brace, 1972; Kirby and Raleigh, 1973; and others). This substitution results in the following formulas:

$$\dot{\varepsilon} = C_1 \sigma \exp(-g^* T_m/T) \tag{2}$$

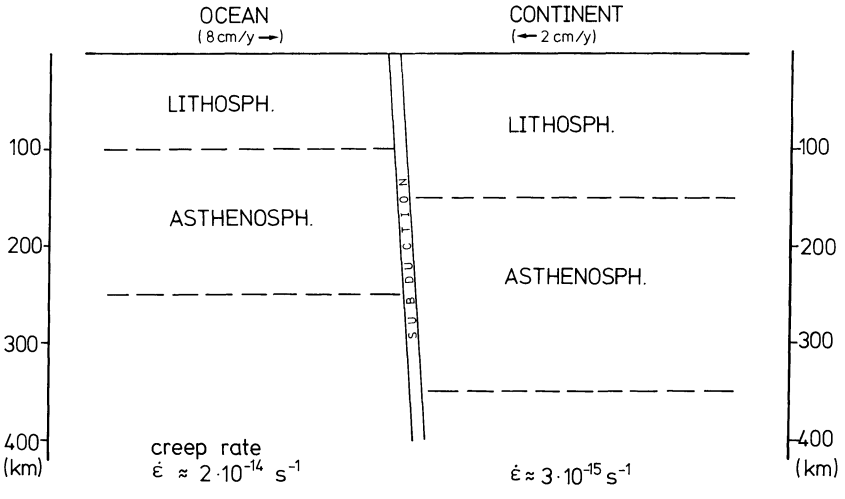

Fig. 1. Plate tectonic model (exaggeration 1:10)

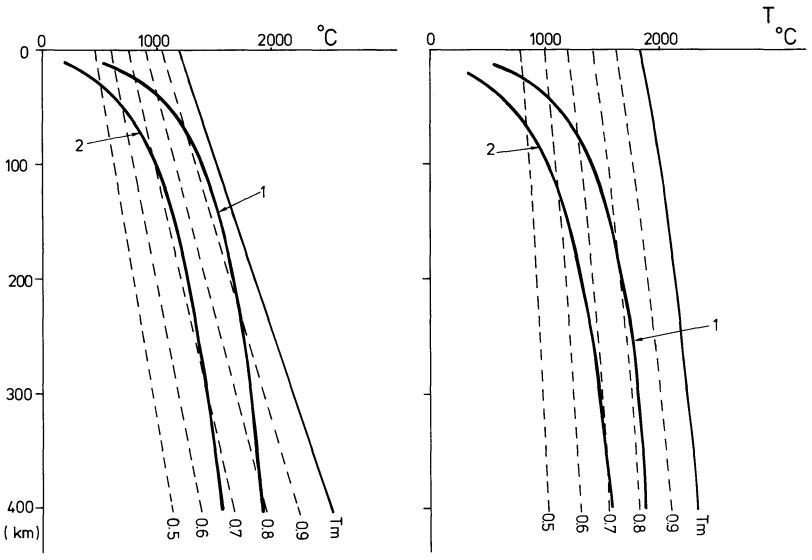

Fig. 2. Temperatures and melting points in the upper 400 km of the earth; *left:* T_m = dry pyrolite solidus (Stocker and Ashby, 1975); *right:* T_m = Forsterite$_{90}$ melting curve (Carter, 1976); 1: hot oceanic geotherm (Griggs, 1972); 2: continental shield geotherm (Clark and Ringwood, 1964); *dashed lines:* fractions of melting point

with

$$C_1 = \alpha_1 \Omega D_0 / r^2 kT \tag{3}$$

and α_1 = constant
k = Boltzmann's constant
r = grain size
Ω = atomic volume
D_0 = diffusion constant
g = constant

which are valid for grain size dependent NH creep and

$$\dot{\varepsilon} = C_3 \sigma^3 \exp(-g^* T_m / T) \tag{4}$$

with

$$C_3 = \alpha_3 \Omega D_0 / \mu^2 kT \tag{5}$$

and α_3 = constant
μ = shear modulus

which are valid for dislocation ($=PL$, $n=3$) creep. For detailed explanations and derivations of these equations see Weertman (1970) and papers 1 and 2.

From a comparison of Equations (2) and (4) it is seen that power law creep with $\dot{\varepsilon} \sim \sigma^3$ is much more sensitive to changes in stress than is NH creep. Using

Equations (2–5) and the relation

$$\eta = \sigma/\dot{\varepsilon} \tag{6}$$

the effective viscosity can be determined on the basis of the "temperature method". That creep process will dominate which gives the highest creep rate in each stress level. In the transition from one creep process to the other, both processes contribute about equally to the resulting creep rate. The transition from *PL* to *NH* creep occurs at ever decreasing stress as the temperature increases and as the grain size decreases (see paper 1, Fig. 4 and paper 2, Fig. 6).

Two different melting point-depth curves will be considered: (a) the dry pyrolite solidus curve, taken from Stocker and Ashby (1973, Fig. 9) and (b) the dry Forsterite$_{90}$ melting curve, taken from Carter (1976, Fig. 39). These two melting curves differ by about 600° C at a pressure of 1 bar and come together in a pressure range of about 100 kb. In Figure 2a and b both melting curves are plotted with the geotherm of a hot oceanic region (Griggs, 1972) and of a continental shield (Clark and Ringwood, 1964). The restriction $T/T_m > 0.5$ for high temperature steady state creep is fulfilled in both cases for depths greater than the crust-mantle boundary.

3. Numerical Values of the Constants Used in the Calculations

As in paper 2, the following numerical values were used in Equations (2–5):

1. The grain size r was taken to be 5 mm according to the observations of mantle specimens, in which most grains lie between 1 and 10 mm. Also indications from the uplift data, as mentioned in paper 2, Figures 4 and 5, give evidence of a grain size around 5 mm. This grain size is taken as constant in the following calculations. Certainly this treatment is a rough approximation because it is well known that grain sizes vary not only with temperature and pressure but also with tectonic stress (Kohlstedt et al., 1976; Mercier, 1977).

2. The constant g^* was examined by Kohlstedt and Goetze (1974) in their laboratory creep experiments on dry olivine; they obtained a best value of $g^* = 29$, which is used here. The experimental values of g^* in olivine creep studies of other authors vary between 26.4 and 31.8 with a mean of 29 (Weertman and Weertman, 1975). Since $g^* \approx 10^3\, Q/RT_m$, one finds an activation energy of $Q \approx 125$ kcal/mol at the melting point $T_m = 2170\,K$ of Fo_{90} at 1 bar. This Q value is also a mean obtained from a number of measurements by different authors (see Goetze, in preparation, Fig. 10) and is nearly constant in the temperature interval from $0.5\,T_m$ to T_m.

If one takes the dry pyrolite solidus temperature T_m (1 bar) $= 1470\,K$, and $g^* = 29$, an activation energy of $Q \approx 85$ kcal/mol results. Schwenn and Goetze (1977) obtained this value as a mean for Coble creep in olivine during hot pressing.

3. The following numbers were used for the constants C_1 and C_3 in Equations (2 and 4): $C_1 = 2 \cdot 10^{-4}$ cm s g^{-1} for T_m, a grain size $r = 5$ mm and $\alpha_1 = 10$ (Weertman, 1970); included in C_1 is the diffusion constant $C_0 = 3 \cdot 10^4$ cm^2 s^{-1}

(Goetze and Kohlstedt, 1973). $C_3 = 4.2 \cdot 10^{11}\,\mathrm{kb}^{-3}\,\mathrm{s}^{-1}$, as experimentally determined by Kohlstedt and Goetze (1974) at the olivine melting point. If $\alpha_3 = 2.26 \cdot 10^{12}\,\mathrm{dyn\,cm}^{-2}$, then the diffusion constant will be $D_0 \approx 10^6\,\mathrm{cm}^2\,\mathrm{s}^{-1}$.

The constants differ from those in paper 1 where a value of $g^* = 18$ was used. This g^* was based on hot creep experiments with different metals (Weertman, 1970) and resulted in a $C_3 = 8.2 \cdot 10^4\,\mathrm{kb}^{-3}\,\mathrm{s}^{-1}$. The g^* and C_3 values from Kohlstedt and Goetze's (1974) experiments on dry olivine crystals seem to be more realistic for the mantle conditions. The difference in the resulting effective viscosity on the base of both mentioned sets of constants is small for temperatures around $0.7\,T_m$, but reaches about one order of magnitude for $0.5\,T_m$ and for T_m.

Introducing the constants in Equations (2), (4), and (6), stresses and effective viscosities for the models are obtained.

4. Results

Figures 3 and 4 show so called deformation maps (=stress-depth curves with the strain rate as a parameter) for the oceanic and continental geotherms from Figure 2. The subduction zone in these figures is considered only as a separating feature and is not specifically investigated in this study. Figures 3a and b are based on the dry pyrolite solidus curve and are taken from paper 2, Figures 7 and 8. Figures 4a and b show the analogous maps based on the Fo_{90} melting curve, maps which are similar to those of Kirby and Raleigh (1973). Using the pyrolite solidus curve one obtains high homologous temperatures T/T_m, especially for the oceanic case; they reach nearly 0.95 below oceans and 0.72 below continents. *NH* creep seems to play an important role below oceans for geologic strain rates, because stresses in this particular model are in general very small. In the deformation map based on the Fo_{90} melting curve (Figs. 4a and b) homologous temperatures reach a maximum of 0.83 for a "hot" oceanic asthenosphere and 0.7 for the continental shield, but at much greater depth than in the case discussed above. Under these conditions, *NH* creep only plays a minor role. Stresses are about a factor of 10 higher than for the dry pyrolite model. These stress values are in good accord with those given by Kirby and Raleigh (1973).

Neugebauer and Breitmayer (1975) also calculated a deformation map for the oceanic mantle to a depth of 1100 km and under the assumption of a power creep law ($n=3$). They adjusted the strain rates to a sinking rate of the plate of 8 cm/y to avoid the use of problematic constants. Their stress values are about 2 orders of magnitude higher than the stresses in this consideration calculated on the base of the Fo_{90} melting curve.

The power creep law ($n=3$) leads to a relation between σ and $\dot{\varepsilon}$ in the form of $\sigma \sim \dot{\varepsilon}^{1/3}$. Therefore stresses could change up to a factor of about 3 if the strain rate changes by about one order of magnitude in a depth range of 400 km. A larger variation of the creep rate does not seem to occur in zones of quiescence, i.e. away from plate boundaries. If one treates *NH* creep as the dominant

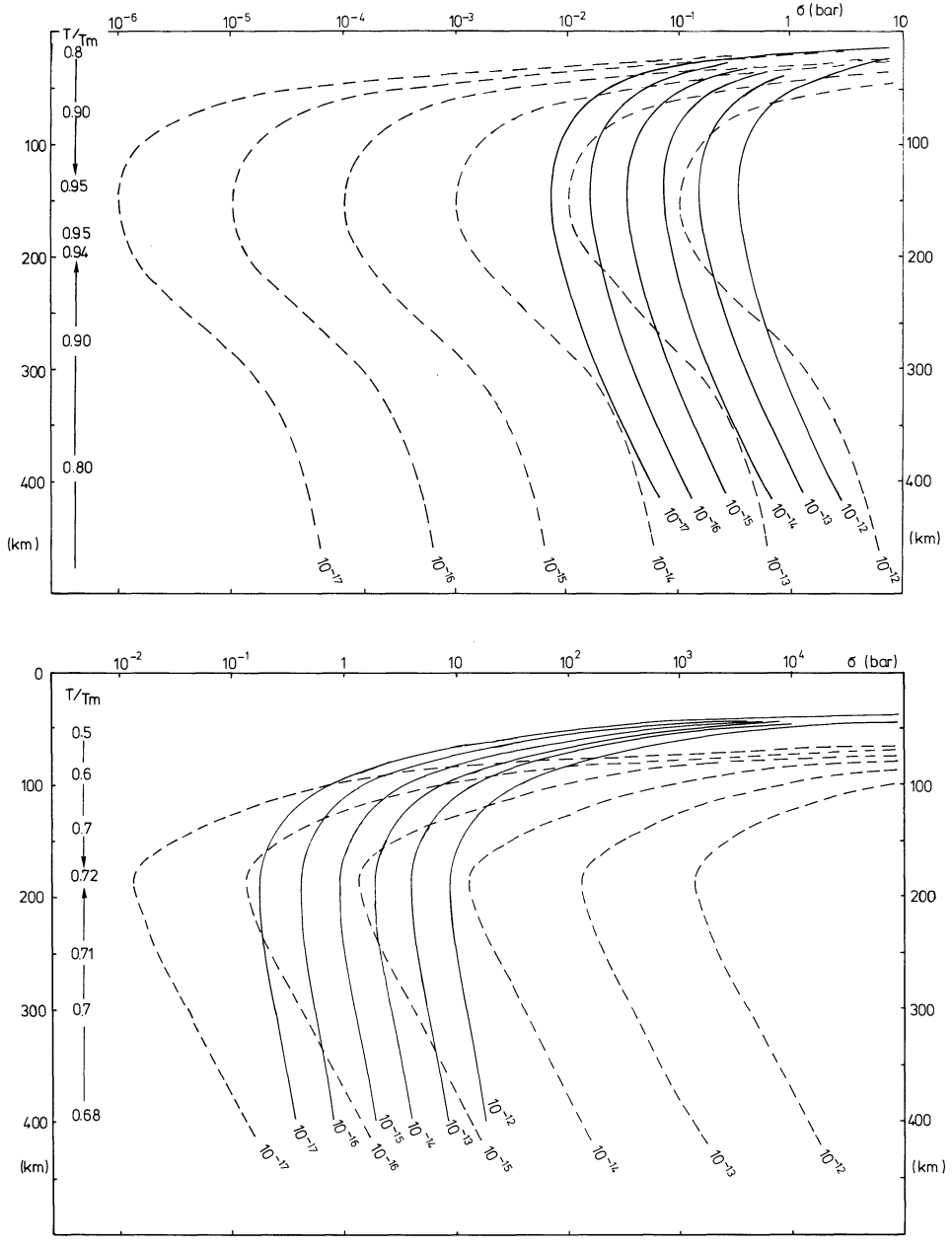

Fig. 3. Stress-depth curves with the strain rate $\dot{\varepsilon}$ as a parameter on the basis of the dry pyrolite solidus curve for an hot ocean (above) and a continental shield (below). Full lines: *PL* creep; dashed lines: *NH* creep; on the left side: the corresponding homologous temperatures

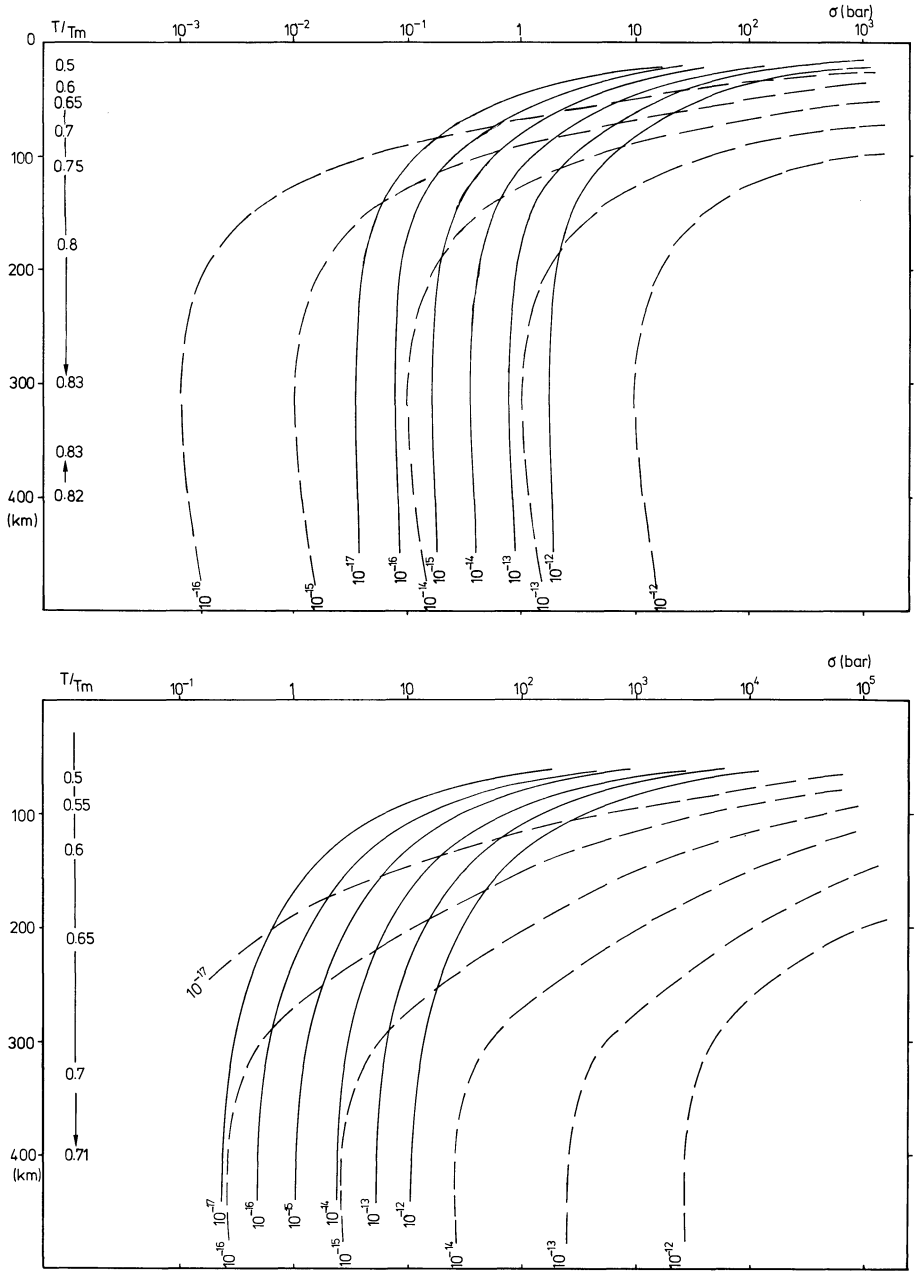

Fig. 4. As Figure 2, but on the basis of the Fo_{90} melting curve

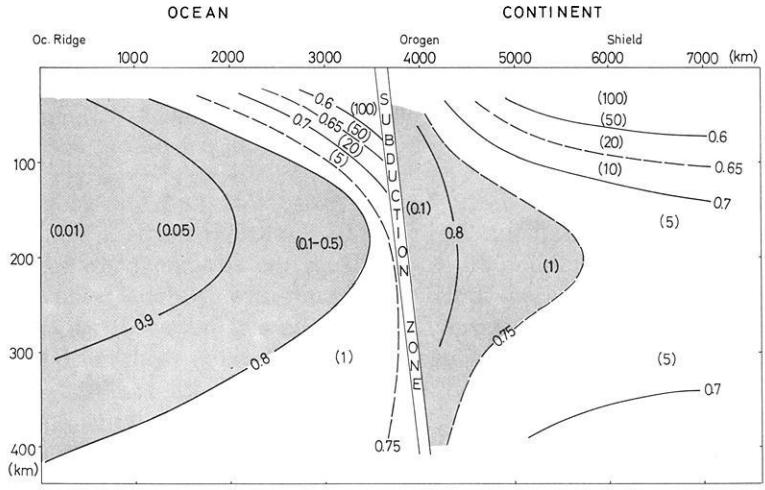

Fig. 5. Average stress distribution and lines of equal homologous temperatures on the basis of the dry pyrolite solidus for the plate tectonic model (Fig. 1). Figures in parentheses: stress values in bar hatched areas: zones of dominating *NH* creep

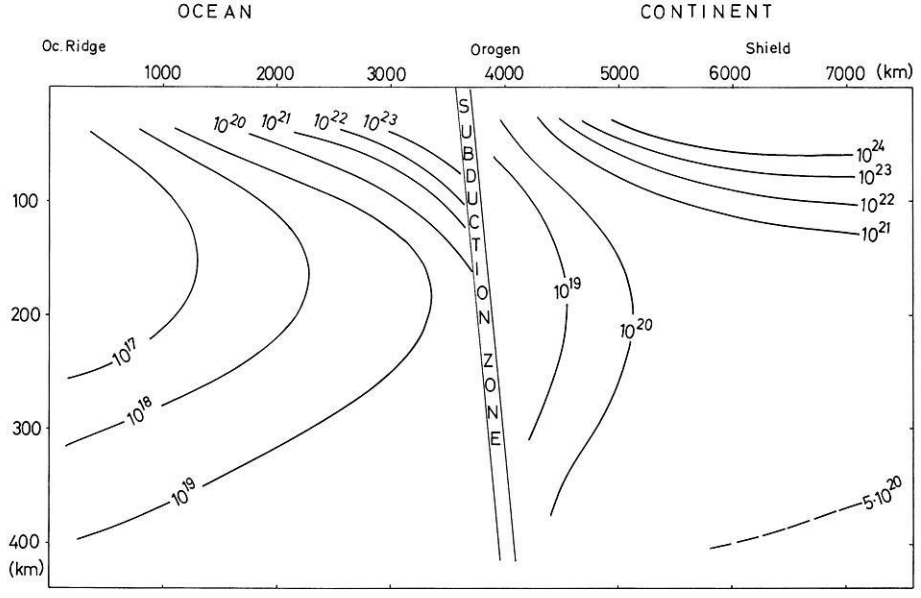

Fig. 6. Viscosity isolines for the case of Figure 5

mechanism stresses will change with the same order of magnitude as the creep rate does.

Figures 5–8 show stresses, homologous temperatures, and effective viscosities for the special plate tectonic model mentioned below. Additional geotherms were used (for instance the Basin and Range temperature distribution, represent-

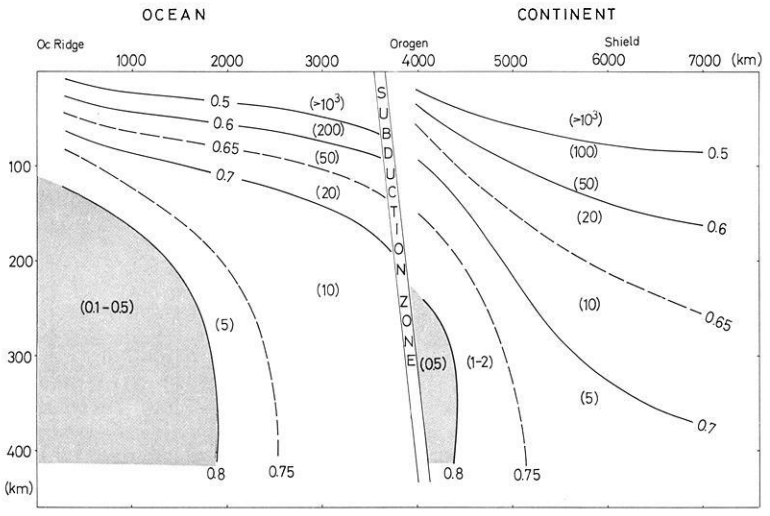

Fig. 7. Average stress distribution and lines of equal homologous temperatures on the basis of the Fo_{90} melting curve; for further legend: see Figure 5

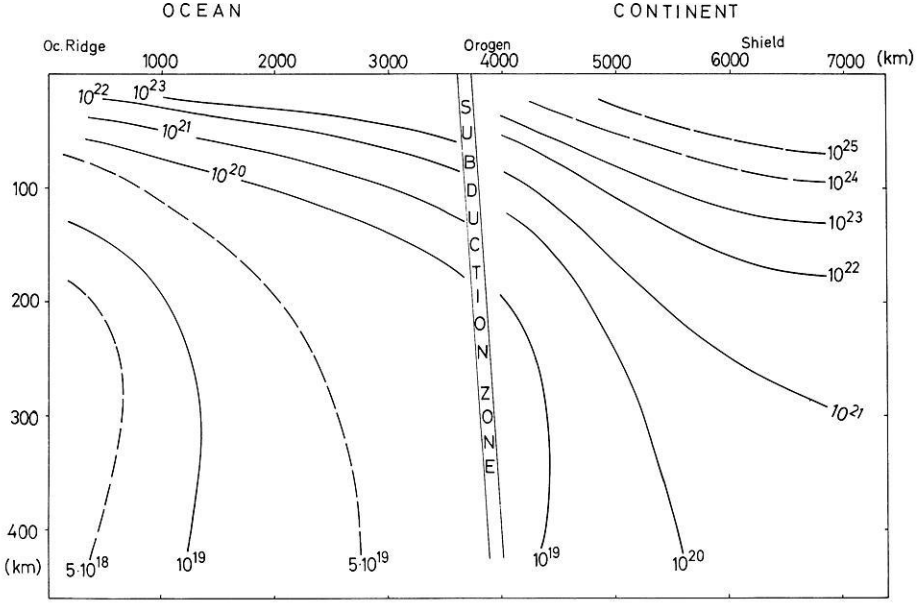

Fig. 8. Viscosity isolines for the case of Figure 7

ing an orogen (Herrin, 1972), and a few oceanic temperature curves of Clark and Ringwood (1974) and Forsyth and Press (1971).

In the plate tectonic model (Fig. 1) the oceanic plate is assumed to be moving with a speed of 8 cm/y. The differential movement may be concentrated in a

layer 100–200 km thick (asthenosphere). From the relationship

$$\dot{\varepsilon} = \partial v / \partial h \approx v/h \tag{7}$$

where h = gliding thickness
and v = drift velocity

a creep rate $\dot{\varepsilon} \approx 2 \cdot 10^{-14}\,\mathrm{s}^{-1}$ results. For the continental plate which is drifting at 2 cm/y a strain rate $\dot{\varepsilon} \approx 3 \cdot 10^{-15}\,\mathrm{s}^{-1}$ is calculated. They represent mean creep rates which may be correct down to the middle of the asthenosphere and will decrease slightly with increasing depth because of increasing pressure (see Eq. (1)). However, this effect is not considered here. The calculated stresses are valid for those zones in the asthenosphere which do not show tectonic activity, for instance for the asthenosphere beneath the deep sea floor and beneath continental shield regions.

In Figures 5 and 7 those zones are indicated in which *NH* creep yields the higher creep rate for a given stress. This is the case in wide regions of the asthenosphere below oceans and also in the region around an orogen below continents for the first case which is based on the dry pyrolite solidus. In the second model, based on the Fo_{90} melting curve, *NH* creep plays only a minor role, locally confined to the vicinity of oceanic ridges (or plumes) and perhaps in small zones below continental orogens. The important difference between the two T_m-models is clearly visible in the stress-depth distribution. Whereas the first model is characterized by very low stresses (below 1 bar in most parts of the oceanic and below 5 bar in most parts of the continental asthenosphere), stresses resulting in the Fo_{90} melting model are higher by one order of magnitude. However, they reach their minimum values at greater depths than in the first model. This stress level (10–100 bar in the upper part of the asthenosphere and 1–2 kb in the lithosphere) is favoured by most authors who have carried out laboratory experiments or electron microscope observations.

A further difference between the models is the "shape" of the asthenosphere. Characteristic of the first model is a pronounced high temperature channel at a depth of 80–250 km under oceans and 130–350 km under continents. In the second model, a pronounced asthenospheric shannel is not indicated; on the contrary, there seems to exist a region of more or less constant temperature from about 200 km down to great depths. Upper mantle models derived from seismic observations indicate the existence of a more or less limited asthenospheric channel, at least below oceans (e.g. Smith, 1972; Forsyth, 1975; Froidevaux et al., 1977). They support the result of model 1 whereas O'Connell (1977) derived a mantle model with a relatively uniform temperature structure in the whole upper mantle without a pronounced asthenospheric channel from glacial rebound data and gravity anomalies. His ideas are in better agreement with the result of model 2. Both these models may limit the realistic mantle temperature variation, if the assumption "dry" is correct.

Figures 6 and 8 show the corresponding viscosity profiles. The calculations were made for *NH* creep with a grain size of 5 mm and for *PL* creep with the stress distribution from Figures 5 and 7. Both melting temperature models show effective viscosity values not very different from each other. The remarkable

difference again is shown in the shape of the viscosity isolines. They delineate the asthenosphere as a 150–300 km broad low viscosity channel in the first model.

In the second model, however, the low viscosity asthenosphere covers the depth range from 150–200 km to at least 400 km, and no indication of a viscosity decrease with increasing depth is seen. A low velocity "channel" which is shown by numerous seismic measurements to be in the depth range of 80 km (ocean) to 300 km (Precambrian shield) must be caused by the existence of minor amounts of water (or other fluid phases) in the upper mantle material, if the Fo_{90} melting temperature model is the realistic one. Obviously, this water content must be more significant below oceans. The dry melting curve may then be partially replaced by a wet melting curve. Green and Liebermann (1976) suggest the existence of a zone of incipient melting ($<2\%$) with an abrupt beginning at about 80–90 km depth below oceans because of amphibole break down connected with a water content $<0.4\%$. Their considerations are based on the pyrolite melting curve. Such a sharp boundary is not confirmed so far by any seismic measurements. Nor is the recording of P_n-velocities larger than $8.5\,\mathrm{km\,s^{-1}}$ at depths of 50–100 km in agreement with a wet pyrolite model. Also Wyllie (1971) has shown the influence of the presence of 0.1% water on the peridotite melting curve. Both investigations show a depression of the melting point by about 500° C at a depth greater than about 100 km. It seems probable that even a smaller water content will change the creep mechanism strongly.

5. Conclusions

Based on the assumption that the lithosphere and asthenosphere are dry, two rheologic models were calculated which provide boundary conditions for creep processes:

Model 1 (based on the dry pyrolite solidus melting-depth curve) indicates that the asthenosphere begins at rather shallow depths and terminates between 300 and 400 km. In model 2 (based on the Fo_{90} melting-depth curve) the asthenosphere begins at a deeper level and extends to greater depths than in model 1, i.e. no changes in the physical parameters are indicated to a depth of 400 km. In general the viscosity values (i.e. the mean effective viscosity of the asthenosphere) are similar in both models. They both show a viscosity difference of about $1^1/_2$ orders of magnitude between the continental and oceanic asthenospheres.

If there is a relation between seismic Q-values and effective viscosity η as suspected by McConnell (1965) and Meissner (1977), seismic investigations should reveal the differences between the asthenospheres below shields and oceans in more detail. Also a discrimination between the dry pyrolite and the Fo_{90} model should be attempted by seismic as well as by mineralogical investigations.

Acknowledgements. I grateful thank Prof. R. Meissner for his stimulating discussions and Dr. A. Binder for correcting my English.

References

Carter, N.L.: Steady state flow of rocks. Rev. Geophys. Space Phys. **14**, 301–360, 1976
Carter, N.L., AvéLallemant, H.G.: High-temperature flow of dunite and peridotite. Bull. Geol. Soc. Am. **81**, 2181–2202, 1970
Carter, N.L., Baker, D.W., George, R.P. Jr.: Seismic anisotropy, flow, and constitution of the upper mantle. In: Flow and Fracture of Rocks, H.C. Heard et al., eds.: AGU, Monogr. **16**, 167–190, 1972
Clark, S.P. Jr., Ringwood, A.E.: Density distribution and constitution of the mantle. Rev. Geophys. Space Phys. **2**, 35–68, 1964
Forsyth, D.W.: The early structural evolution and anisotropy of the oceanic upper mantle. Geophys. J. **43**, 103–162, 1975
Forsyth, D.W., Press, F.: Geophysical tests of petrological models of the spreading lithosphere. J. Geophys. Res. **76**, 7963–7979, 1971
Froidevaux, C., Schubert, G., Yuen, D.A.: Thermal and mechanical structure of the upper mantle: comparison between continental and oceanic models. Tectonophysics **37**, 233–246, 1977
Goetze, C., Brace, W.F.: Laboratory observations of high-temperature rheology of rocks. Tectonophysics **13**, 583–600, 1972
Goetze, C., Kohlstedt, D.L.: Laboratory study of dislocation climb and diffusion in olivine. J. Geophys. Res. **78**, 5961–5971, 1973
Green, D.H., Liebermann, R.C.: Phase equilibria and elastic properties of a pyrolite model for the oceanic upper mantle. Tectonophysics **32**, 61–92, 1976
Green, H.W., Radcliffe, S.V.: Deformation processes in the upper mantle. In: Flow and Fracture of Rocks, H.C. Heard et al., eds.: AGU, Geoph. Monogr. **16**, 139–156, 1972
Griggs, D.T.: The sinking lithosphere and the focal mechanism of deep earthquakes. In: Nature of the Solid Earth, E.C. Robertson, ed., pp. 361–384. New York: McGraw Hill 1972
Herring, E.: A comparative study of upper mantle models: Canadian shield and Basin and Range provinces. In: Nature of the Solid Earth, E.C. Robertson, ed., pp. 216–231. New York: McGraw Hill 1972
Herrin, C.: Diffusional viscosity of a polycrystalline solid. J. Appl. Phys. **21**, 437–445, 1950
Kirby, St.H., Raleigh, C.B.: Mechanism of high-temperature, solid state flow in minerals and ceramics and their bearing on the creep behavior of the mantle. Tectonophysics **19**, 165–194, 1973
Kohlstedt, D.L., Goetze, C.: Low-stress high-temperature creep in olivine single crystals. J. Geophys. Res. **79**, 2045–2051, 1974
Kohlstedt, D.L., Goetze, C., Durham, W.B.: Experimental deformation of single crystal olivine with application to flow in the mantle. In: The Physics and Chemistry of Minerals and Rocks, S.K. Runcorn, ed., pp. 35–49. London: J. Wiley & Sons Ltd. 1976
McConnell Jr., R.K.: Isostatic adjustment in a layered earth. J. Geophys. Res. **70**, 5171–5191, 1965
Meissner, R.: Lunar viscosity models. Phil. Trans. Roy. Soc. London, Ser. A, **285**, 463–467, 1977
Meissner, R.O., Vetter, U.R.: Isostatic and dynamic processes and their relation to viscosity. Tectonophysics **35**, 137–148, 1976
Mercier, J.C., Anderson, D.A., Carter, N.L.: Stress in the lithosphere: inferences from steady state flow of rocks. Pure Appl. Geophys. **115**, 199–226, 1977
Neugebauer, H.J., Breitmayer, G.: Dominant creep mechanism and the descending lithosphere. Geophys. J. **43**, 873–895, 1975
Nicolas, A.: Flow in upper mantle rocks: some geophysical and geodynamic consequences. Tectonophysics **32**, 93–106, 1976
Nicolas, A., Bouchez, J.L., Boudier, F., Mercier, J.C.: Textures, structures, and fabrics due to solid state flow in some European lherzolites. Tectonophysics **12**, 55–86, 1971
O'Connell, R.J.: On the scale of mantle convection. Tectonophysics **38**, 119–136, 1977
Phakey, P., Dollinger, G., Christie, J.: Transmission electron microscopy of experimentally deformed olivine crystals. In: Flow and Fracture of Rocks, H.C. Heard et al., eds. AGU, Geophys. Monogr. **16**, 117–138, 1972
Post, R.L. Jr., Griggs, D.T.: The earth's mantle: evidence of non-Newtonian flow. Science **181**, 1242–1244, 1973
Raleigh, C.B., Kirby, S.H.: Creep in the upper mantle. Mineral. Soc. Am., Spec. Papers **3**, 113–121, 1970

Schwenn, M.B., Goetze, C.: Creep of olivine during hot-pressing. Tectonophysics, in press, 1977
Sherby, O.D., Simnad, M.T.: Prediction of atomic mobility in metallic systems. Trans. Am. Soc. Metals, **54**, 227–240, 1961
Smith, S.W.: The anelasticity of the mantle. Tectonophysics **13**, 601–622, 1972
Stocker, R.L., Ashby, M.F.: On the rheology of the upper mantle. Rev. Geophys. Space Phys. **11**, 391–426, 1973
Twiss, R.J.: Structural superplastic creep and linear viscosity in the earth's mantle. Earth Planet. Sci. Lett. **33**, 86–100, 1976
Vetter, U.R., Meissner, R.O.: Creep in geodynamic processes. Tectonophysics, **42**, 37–54, 1977
Weertman, J.: The creep strength of the earth's mantle. Rev. Geophys. Space Phys. **8**, 145–168, 1970
Weertman, J., Weertman, J.R.: High temperature creep of rock and mantle viscosity. Ann. Rev. of Earth and Plan. Sci., **3**, 293–315, 1975
Wyllie, J.P.: Role of water in magma generation and initiation of diapiric uprise in the mantle. J. Geophys. Res. **76**, 1328–1338, 1971

Received June 1, 1977/Revised Version October 7, 1977